Available online at www.sciencedirect.com

SCIENCE DIRECT®

Chemical Physics Letters 379 (2003) 507–511

CHEMICAL PHYSICS LETTERS

www.elsevier.com/locate/cplett

Light-induced luminescent enhancement and structural change in cubic nanocrystallineY_2O_3:Tb

Jiwei Wang *, Hongwei Song *, Baojuan Sun, Xinguang Ren, Baojiu Chen, Wu Xu

Key Laboratory of Excited State Physics, Changchun Institute of Optics, Fine Mechanics and Physics,
Chinese Academy of Sciences, 140 People Street, Changchun 130022, PR China

Received 5 April 2003; in final form 11 July 2003

Abstract

Light-induced spectral change and its restore process in the dark of nanocrystalline Y_2O_3:Tb were studied. It was observed that the intensity in 4f5d band increased by ultraviolet and visible irradiation. The smaller the particle size and the shorter the wavelength is, the larger the light-induced luminescent enhancement is. Two restore components were observed, corresponding to two defects, the internal and the surface. The studies on electron spin resonance (ESR) spectra indicate that optical irradiation eliminated the dangling Y–O bonds in the surface.

1. Introduction

Lanthanide-doped yttrium (Y_2O_3) are common phosphors in optical display and lighting applications, and the search for new phosphors has led to the preparation of nanocrystalline forms of Y_2O_3 [1]. Over the past decade, much attention has been given to two well-known phosphors, Y_2O_3:Eu^{3+} and Y_2O_3:Tb^{3+} [2–4]. As is well known, the reduction of particle size of crystalline systems leads to important modifications of some of their bulk properties due to the following special electronic properties of nanometer particles: (1) the quantum size effect and (2) the increase of surface to volume ratio [5–7]. It is expected that the luminescent quantum efficiency (QE) in nanoparticles be enhanced due to the quantum size effect. Unfortunately, the real QE in nanoparticles generally decreases due to unexpected surface effects. To improve the QE in nanoparticles, the surface effects should be well studied. However, the origin of surface defects and its influence on electronic transitions have not been well understood up to now.

In this Letter, to understand the surface effects in yttrium nanoparticles, the light-induced luminescent enhancement and electron spin resonance (ESR) spectra were studied. The light-induced luminescent enhancement in nanoparticles was first reported in ZnS:Mn and since then it became a helpful method to study surface effects [8]. In

---

* Corresponding authors. Fax: +86-4316176317.
E-mail addresses: Jwwang68@sohu.com.cn (J. Wang), Songhongwei2000@sina.com.cn (H. Song).

0009-2614/$ - see front matter © 2003 Elsevier B.V. All rights reserved.
doi:10.1016/j.cplett.2003.08.011

Y_2O_3:Tb nanoparticles, light-induced luminescent enhancement was also observed [9]. EPR spectrum is a powerful technique to reveal structural defects [10–12].

2. Experiments

The Y_2O_3:Tb nanocrystals were prepared by combustion. In the preparation, Y_2O_3 and Tb_4O_7 were dissolved in nitric acid and glycine was dissolved in distilled water, then the two kinds of solutions were mixed together to form the precursor. The solution was concentrated by heating until excess free water evaporated and spontaneous ignition occurred. The resultant Y_2O_3:Tb (1 mol%) powders were formed after the combustion was finished. The particle size was controlled by the ratio of glycine to $Y(NO_3)_3$. To improve crystallinity, the nanocrystalline powders were all heat-treated at 500 °C for 1 h. The bulk Y_2O_3:Tb powders (~2 μm) were formed by annealing at 1200 °C for 6 h [14,15].

The excitation and emission spectra were measured with a Hitachi F-4500 fluorescence spectrometer. The continuous lights separated from a xenon-lamp were used for irradiation source, with a line width of 10 nm and power density of 10–100 μW/cm^2. The ESR spectra were measured by a GAES-FE3AX ESR spectrometer. It was with a central magnetic field strength of 3363 G, scanning scope of 5000 G, multiplying factor of 5000 G and was calibrated with DPPH. All the experiments were performed at room temperature.

3. Results and discussion

Fig. 1 shows X-ray diffraction patterns of the nanocrystalline Y_2O_3:Tb powders. It can be seen that all the nanoparticles exhibit pure cubic structure. The particle sizes were estimated by the half width of the diffraction peaks in the light of Scherrer formula [13] to be 35, 50 and 70 nm corresponding to the molar ratios (glycine to $Y(NO_3)_3$) of 1.45, 1.55 and 1.67.

Fig. 2 shows the $^5D_4$–^7F_J emissions measured before and after irradiation in the 35-nm powders.

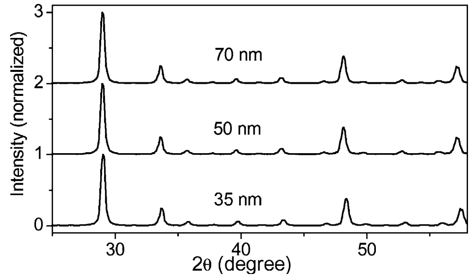

Fig. 1. XRD-patterns in different Y_2O_3:Tb.

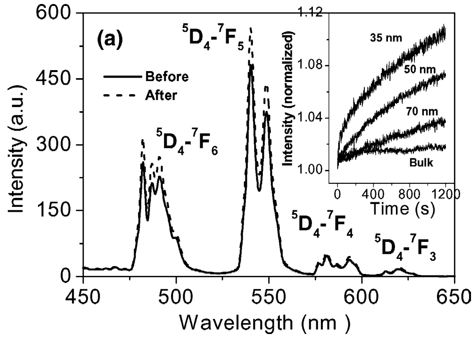

Fig. 2. Emission spectra before and after irradiation at 250 nm for 40 min ($\lambda_{ex} = 275$ nm) in the 35-nm Y_2O_3:Tb. Inset: dependence of normalized emission intensity at 542 nm on irradiation time ($\lambda_{ir} = 250$ nm).

It appears that the emission intensity increased after irradiation. Actually, in the other samples the emission intensity also increased by irradiation. The inset shows the dependence of normalized emission intensity at 542 nm on irradiation time in different nanoparticles. The intensity growth dynamics was well fitted by a function of $[1 + \alpha(1 - \exp(-\beta t))$, where α presents the saturation growth intensity and β presents the intensity change rate. By fitting, the values of α in the 35, 50, 70 nm and the bulk powders were determined to be 0.10, 0.08, 0.04 and 0.02, respectively. It is apparent that the smaller the nanocrystal size is, the larger the relative change is. It is interesting to note that unlike Y_2O_3:Tb, the excited charge transfer (CT) band in Y_2O_3:Eu decreased by irradiation. This was attributed to different excitation mechanisms [14].

Fig. 3a shows the excitation spectra at 542 nm at different aging time. In Fig. 3a, the peak at

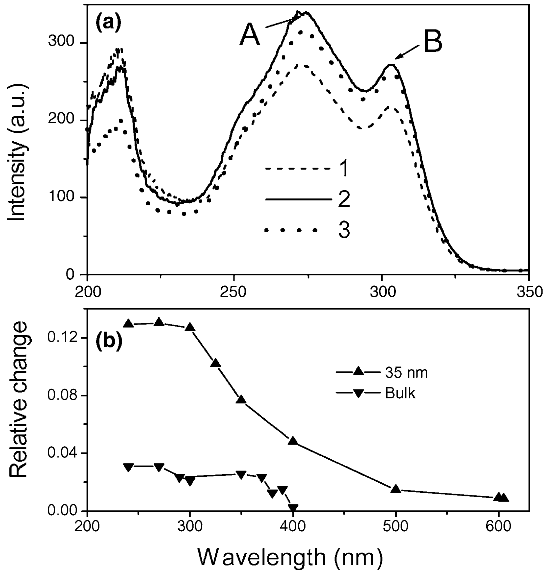

Fig. 3. (a) Excitation spectra measured at different aging time in the 35-nm Y_2O_3:Tb. 1 – before irradiation; 2 – immediately after irradiation at 290 nm for 40 min; 3 – after the irradiation light was shut off 64 h. (b) Dependence of relative intensity change of the 4f5d excitation band on irradiation wavelength.

210 nm is associated with the energy transfer (ET) excitation from the Y_2O_3 host to Tb^{3+} [14]. The bands extended from 235 to 350 nm are assigned to the 4f5d transitions. The 4f5d bands contain two peaks, A and B. It can be seen that after 290-nm irradiation the intensity in the 4f5d band increased, while that in the ET band had little variation. As the irradiation light was shut off, the intensity in the 4f5d band increased again and tended to restore to its original state. Two points should be mentioned here: (1) The intensity in ET band also increased as the wavelength of irradiation light was corresponding to the ET band (200–235 nm). (2) The intensity in peak A restored faster than that in peak B. Fig. 3b shows the relative intensity change in the 4f5d excitation band as a function of wavelength of the irradiation light. It appears that the longer the wavelength is, the smaller the relative intensity change is, for both the nanometer and the bulk particles. As the wavelength of irradiation light increases to a certain value, the intensity change is nearly zero. This wavelength is called as cut-off wavelength. In the bulk powders the cut-off wavelength is ~400 nm, while in the 35-nm powders it extends to ~600 nm.

Fig. 4 shows the dependence of relative change in 4f5d bands as a function of recovery time in different powders. In Fig. 4, the relative intensity change was determined by the equation of $[I_a(t) - I_b]/[I_a(0) - I_b]$, where I_b is the intensity measured before irradiation, $I_a(0)$ is the intensity measured immediately after the irradiation light was shut off, $I_a(t)$ is the intensity measured after the irradiation light was shut off t hours. It can be observed that for the nanoparticles, two recovery components exist, one faster and one slower. The recovery time constant of the faster component is 8.6 h and the ratio of the component is 40%. The recovery time constant of the slower component is much longer than several ten hours. For the bulk powders, only one faster component exists, with a recovery time constant of 3.8 h.

The dark recovery time constant is dominated by the thermal activation rate between the changed and unchanged states. The appearance of two recovery time constants suggests that there exist two thermal activation rates between the changed and unchanged states, which correspond to two kinds of structural changes. In comparison with the recovery processes of the bulk powders, we suggest that the faster recovery component for the nanoparticles is corresponding to internal structural change, while the slower component to the surface

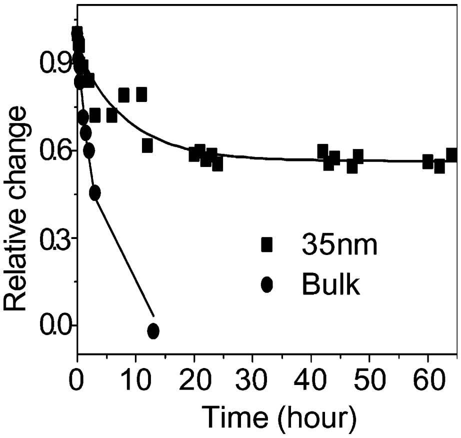

Fig. 4. Relative intensity change of 4f5d bands as a function of recovery time in the dark.

structural change. Dhanaraj et al. studied the thermally stimulated luminescence of Y_2O_3:Eu. They observed a thermally stimulated luminescence glow peak at 420 °C in the nanocrystalline Y_2O_3:Eu powder, while observed a glow peak at 135 °C in the bulk powder [15]. This means that the thermal activation energy of electrons trapped in surface defects is larger than that trapped in the internal defects, which strongly supports our present result.

Suppose that the luminescent enhancement is related to the electron trapping of defects, and the recovery process to the thermal activation of trapped electrons. Two defects, surface and internal, contribute to the luminescent enhancement. Then the recovery process for the nanoparticles can be easily deduced as

$$\Delta I \propto n_s \exp(-v_s t) + n_i \exp(-v_i t),$$

where ΔI is the relative change of total intensity, n_s and n_i are, respectively, the number of electrons trapped in surface and internal defects, v_s and v_i are the thermal activation rates of electrons in the surface and internal defects, respectively. By fitting the experimental results in Fig. 4, n_s/n_i in nanoparticles was deduced to be 1.5, v_i to be 3.3×10^{-5} s^{-1}, v_s is much smaller than v_i. In the bulk powders, n_s is much smaller than n_i, thus the luminescent change restores exponentially in the dark. v_i was deduced to be 7.3×10^{-5} s^{-1}.

Fig. 5 shows the ESR spectra in different samples. In the bulk powders it is hardly to observe any ESR signal. In the undoped Y_2O_3 nanocrystals, a weaker signal appeared between 3000 and 3500 G. It is assigned to be unshared electron pair of nanocrystalline Y_2O_3 caused by surface defects. According to the width and shape of the signal, we suggest that it originates from metal ions. Considering the compositions of the host, it was attributed to the dangling bonds of yttrium. The existent of yttrium dangling bonds means the existent of the oxygen vacancies in the surface. In the nanocrystalline Y_2O_3:Tb without irradiation, besides the similar signal caused by the dangling bonds of yttrium, a stronger signal varying from 1300 to 1600 G was observed. This signal was assigned to the ESR signal of Tb^{4+}[16]. It can be seen that the strength of the signal caused by Tb^{4+} did not change by irradiation, indicating that the valence state of terbium did not change. On the other hand, the signal caused by the dangling bonds of yttrium nearly disappeared after irradiation, indicating that most of the surface oxygen vacancies were optically filled. We suggest that it is the surface oxygen vacancies taking as nonradiative relaxation channels. Thus the optical filling of oxygen vacancies leads to the luminescent enhancement of Tb^{3+}.

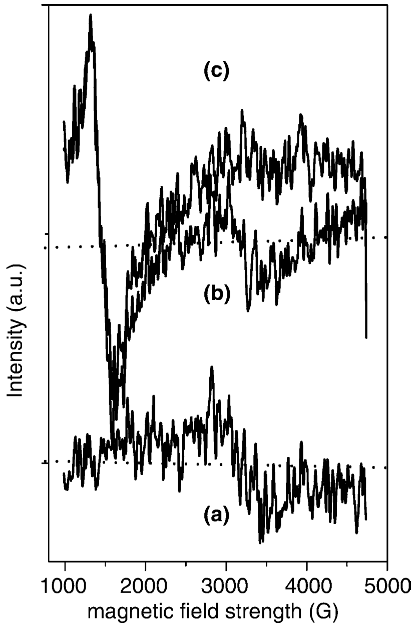

Fig. 5. ESR spectra of different nanocrystalline Y_2O_3 powders: (a) undoped Y_2O_3; (b) Tb-doped Y_2O_3; (c) Tb-doped Y_2O_3 with 325-nm exposure.

4. Conclusions

The dependence of light-induced spectral change on particle size, irradiation time and wavelength was studied. It can be concluded that the smaller the particle size and the shorter the wavelength is, the larger the intensity change is. The recovery processes of the change in the dark were also studied. Two recovery time constants in the dark were observed in the nanoparticles, while only one shorter constant was observed in the bulk powders. This suggests that the intensity change with shorter recovery time is contributed by internal defects, while the change with longer recovery time is contributed by surface defects. EPR spectra were studied to reveal the structural change in/near the surface. It was concluded that the optical irradiation eliminated the dangling Y–O bonds in the surface.

Acknowledgements

This work was supported by 'One Hundred Talents Project' of Chinese Academy of Sciences (Z01M20).

References

[1] D.K. Williams, B. Bihari, B.M. Tissue, J.M. McHale, J. Phys. Chem. B 102 (1998) 916.
[2] K.S. Hong, R.S. Meltzer, B. Bihari, D.K. Willliams, B.M. Tissue, J. Lumin. 76&77 (1998) 234.
[3] Y.L. Soo, S.W. Huang, Z.H. Ming, Y.H. Kao, G.C. Smith, E. Goldburt, R. Hodel, B. Kulkarri, J.V.D. Veliadis, R.N. Bhargava, J. Appl. Phys. 83 (1998) 5404.
[4] R.N. Bhargava, V. Chhabra, B. Kulkarni, J.V. Veliadis, Phys. Stat. Sol. B 210 (1998) 621.
[5] R.N. Bhargava, D. Gallagher, X. Hong, A. Nurmikko, Phys. Rev. Lett. 72 (1994) 416.
[6] A. Trave, F. Buda, A. Fasolino, Phys. Rev. Lett. 77 (1996) 5405.
[7] J.R. Agger, M.W. Anderson, M.E. Pemble, O. Terasaki, Y. Nozue, J. Phys. Chem. B 102 (1998) 3345.
[8] J. Yu, H. Liu, Y. Wang, F.E. Fernandez, W. Jia, L. Sun, C. Jin, D. Li, J. Liu, S. Huang, Opt. Lett. 22 (1997) 913.
[9] Goldburt et al., J. Soc. Inf. Display 4 (1996) 365.
[10] W.L. Warren, P.M. Lenahan, S.E. Curry, Phys. Rev. Lett. 65 (1990) 207.
[11] T. Wang, L.D. Zhang, X. Fan, J. Appl. Phys. 74 (10) (1993) 6313.
[12] D. Jouse, J. Kanicki, J.H. Stachic, Appl. Phys. Lett. 54 (11) (1989) 13.
[13] Y. Tao, G. Zhao, W. Zhang, S. Xia, Mater. Res. Bull. 32 (1997) 501.
[14] H. Song, B. Chen, H. Peng, J. Zhang, Appl. Phys. Lett. 81 (2002) 1776.
[15] J. Dhanaraj, R. Jagannathan, T.R.N. Kutty, C.-H. Lu, J. Phys. Chem. B 105 (2001) 11098.
[16] A.M. Ziatdindv, in: First Asia-Pacific EPR/ESR Symposium, June, vol. 19, 1997, P31.